Aerosol Optical Thickness over the Oceans Derived from GMS-5 during Spring 2002 and 2003

Kazuhiko MASUDA, Yuzo MANO, Hiroshi ISHIMOTO

Meteorological Research Institute, Tsukuba, Japan

Nozomu OKAWARA, Yoshito YOSHIZAKI

Meteorological Satellite Center, Kiyose, Tokyo, Japan

(Manuscript received 21 July 2004, in final form 4 February 2005)

Abstract

Daily and monthly aerosol optical thickness (AOT) over the ocean, derived from the Geostationary Meteorological Satellite (GMS-5) visible data, were compared with those determined from the sun photometer measurements in March and April 2002. Time variations in the daily AOT derived from the GMS-5 showed good agreements with those from the sun photometer measurements. Correlation coefficient between the GMS-5 and the sun photometer derived daily AOTs was 0.85 for 61 samples taken at three sun photometer observation sites; Ryori, Yonagunijima, and Minamitorishima in Japan. The difference of monthly AOT, the GMS-5 minus the sun photometer, in March and April 2002 were −0.03 and 0.03 at Ryori, −0.01 and 0.18 at Yonagunijima, and 0.01 and 0.07 at Minamitorishima, respectively.

Monthly regional AOT, defined as the median of the daily AOTs over 30° latitude × 30° longitude region, was calculated in latitude from 60°N to 60°S and in longitude from 80°E to 160°W for March and April of 2002 and 2003. In the southern hemisphere, monthly regional AOT was less than 0.1; about 0.1∼0.2 in 0°N∼30°N; larger than 0.2 in 30°N∼60°N with a maximum of 0.4∼0.5 in the western region near the Asian continent. AOTs in 2003 were generally smaller than those in 2002 in six regions between 110°E and 160°W of the northern hemisphere, where aerosol loading is most likely affected by the Asian dust. The numbers of regions, in which the AOT increased/decreased/equivalent from 2002 to 2003, were 3/8/1 in March and April, with the AOT changes from 2002 to 2003 to be as large as −0.04∼0.03.

1. Introduction

Atmospheric aerosols play an important role in the Earth's radiation budget, directly by scattering and absorbing solar and terrestrial radiation and indirectly by changing cloud properties (d'Almeida et al. 1991). Accurate evaluation of the effect of aerosols on the climate requires global information on aerosol properties. Such global information can only be acquired using satellite remote sensing.

Optical thickness of the Asian dust aerosols over the ocean near Japan has been successfully retrieved from the Geostationary Meteorological Satellite (GMS-5) visible measurements during the first intensive observation period (IOP-1), conducted as a part of the Japanese-China joint project on Aeolian Dust Experiment on Climate impact (ADEC) (Mikami et al. 2002), by taking the nonsphericity of dust particles into account. The hourly retrieved optical thicknesses were compared with those derived from the ground based radiometer measurements; sun photometers and sky

Corresponding author: K. Masuda, Meteorological Research Institute, Tsukuba, Ibaraki, 305-0052, Japan.
E-mail: masuda@mri-jma.go.jp

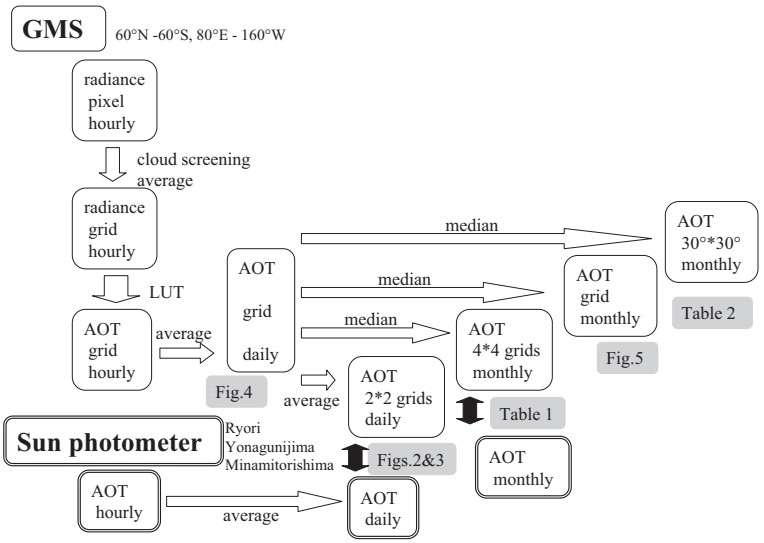

Fig. 1. Schematic overview of the GMS-5 and the sun photometer data processing.

radiometers. The mean and the standard deviation of the optical thickness difference, the GMS-5 minus the radiometers, were −0.03 and 0.17, respectively, for 85 samples where the optical thickness ranges from 0.25 to 1.07 (Masuda et al. 2003).

However, it is not apparent how large errors are included when we apply the inversion scheme for retrieving aerosol optical thickness (AOT) over the whole ocean area observed by the GMS-5, because the aerosol model has been optimized to simulate dust particles in the inversion scheme (Masuda et al. 2002b, 2003). In this paper, we examine the feasibility of retrieving AOT over the ocean from the GMS-5 visible measurements. The daily and the monthly AOTs derived from the GMS-5 are compared with those from the sun photometer measurements made by the Japan Meteorological Agency.

The AOT inversion method from the GMS-5 measurements is outlined in Section 2, together with a brief description of the sun photometer measurements. In Section 3, the daily and the monthly AOTs derived from the GMS-5 and the sun photometers are compared, and the regional monthly AOTs in March and April of 2002 and 2003 are presented. Retrieval errors included in the inversion method are examined in Section 4, in terms of the atmospheric model assumptions.

2. Measurements and inversion method

Schematic overview of the GMS-5 and the sun photometer data processing described in this paper is illustrated in Fig. 1.

2.1 Geostationary Meteorological Satellite

The hourly GMS-5 visible data (6 bit digitization, 0.55∼0.9 μm wavelength, 1.25 km pixel size at nadir) are used for retrieving AOT in daytime, from 09 to 15 in Japanese standard time (JST, Universal Time + 9). A look-up table approach is adopted to convert satellite measurements to AOT. The atmosphere-ocean model and the inversion scheme have been described in Masuda et al. (2002b). The atmosphere-ocean model is outlined in the following paragraphs.

A plane-parallel and vertically inhomogeneous atmosphere is simulated by four homogeneous sub-layers (0 to 2 km, 2 to 5 km, 5 to 13 km, and 13 to 100 km). Aerosols composed of mineral dust particles are assumed to exist in the second layer (2∼5 km), neglecting other types of aerosols for simplicity. The ocean surface is simulated by multiple facets whose slopes vary with the wind speed over the ocean (Cox and Munk 1954). The ocean wind speed is assumed to be 5 m s^{-1}. The radiation from the ocean body is neglected. The inversion could be, therefore, perturbed by a not-so-well-known marine signal.

The optical thickness of the atmospheric molecular scattering and absorption for the mid-latitude summer model, of which the column water vapor amount is 2.9 cm, is obtained from LOWTRAN7 (Kneizys et al. 1988). To include the absorption effect by water vapor into the radiative transfer calculation, a two-term exponent sum fitting approximation was adopted.

The bimodal log-normal aerosol size distribution is assumed where the log-normal function is expressed by $\mathrm{d}n(r)/\mathrm{d}r = [(2\pi)^{1/2} r \ln \sigma]^{-1} \cdot \exp[-(\ln r - \ln r_m)^2/2 \ln^2 \sigma]$. The mode radius ($r_m$) and σ are 0.044 μm and 1.96 for the small component, 0.37 μm and 2.37 for the large component as in Higurashi and Nakajima (1999). The fractions of small and large particle components are chosen so that the resultant Ångström exponent may be 0.47. The complex refractive index is assumed to be 1.50-i0.005. Single scattering phase functions are computed by the semi-empirical theory by Pollack and Cuzzi (1980), taking the nonsphericity of dust particles into account. The nonsphericity parameters are $(r, x_0, G) = (1.1, 7, 10)$ according to Nakajima et al. (1989). Nine optical thickness at $\lambda = 500$ nm (τ_{500}) are considered to be 0.0, 0.02, 0.04, 0.08, 0.16, 0.32, 0.64, 1.28, and 2.56.

A look-up table composed of upward reflectance at the top of the atmosphere is created with four parameters: the solar zenith angle (θ), the satellite zenith angle (θ_0), the azimuth difference angle between solar and satellite directions ($\phi - \phi_0$), and τ_{500}. The reflectance is defined as $\pi I/(F_0 \cos \theta_0)$, where I and F_0 are the upward radiance at the top of the atmosphere and the extraterrestrial incident solar flux density, respectively.

The hourly satellite data from 09 JST to 15 JST are converted to AOT at every 0.25° interval grid point over the ocean. Within the area of ±0.125° in latitude and in longitude for each grid point, cloud screening was performed to extract clear sky pixels. The cloud screening algorithm is almost the same as that used in GMS SST retrieval. Then, the spatially averaged clear sky radiance at each grid is converted to AOT referring to the look-up table. The digitization errors in the GMS-5 radiance measurements would be greatly reduced by the above-mentioned averaging process. Only the grid points with both θ and θ_0 less than 65° are processed to avoid possible errors arising from the observation in large slant directions. The hourly optical thicknesses are averaged to create daily AOT.

2.2 *Sun photometer*

Sun photometer measurements are made in a routine manner by the Japan Meteorological Agency at three observation sites; Ryori (39.0°N, 141.8°E), Yonagunijima (24.5°N, 123.0°E), and Minamitorishima (24.3°N, 154.0°E). The sun photometer measures direct solar radiation in five spectral bands (368, 500, 675, 778, and 862 nm). AOT is derived from the measurements of the total optical thickness by subtracting Rayleigh and gaseous absorption components. The monthly mean of AOT together with the hourly AOT until 2002 are reported in Japan Meteorological Agency (JMA 2004).

3. Results

3.1 *Daily aerosol optical thickness*

Figure 2 shows comparisons of the daily AOTs derived from the GMS-5 with those determined from the sun photometer measurements. It should be noted that the sun photometer observation sites are not located in the ocean area. Furthermore, the observation time of the GMS-5 and the sun photometers are different from each other. To compare the daily AOTs, the following pre-processings were performed. For the GMS-5, a 2×2 grid area was selected near the sun photometer observation site to examine spatial stability of AOT. If the maximum AOT is larger than the minimum AOT + 0.2 in the area, the daily AOT was not calculated, and otherwise, AOT was obtained by averaging 4 AOTs. For the sun photometer, the hourly AOTs at the 500 nm spectral band, reported in JMA (2004), were averaged to obtain the daily AOT. Note that the hourly data are included for selected days and the maximum number of the hourly data is three per day in the JMA report. The daily AOTs are plotted in Fig. 2 only when they are determined in both the GMS-5 and the sun photometer measurements. The daily AOT derived from the GMS-5 shows similar time variations to those from the sun photometer measurements.

Figure 3 shows scatter plots of three obser-

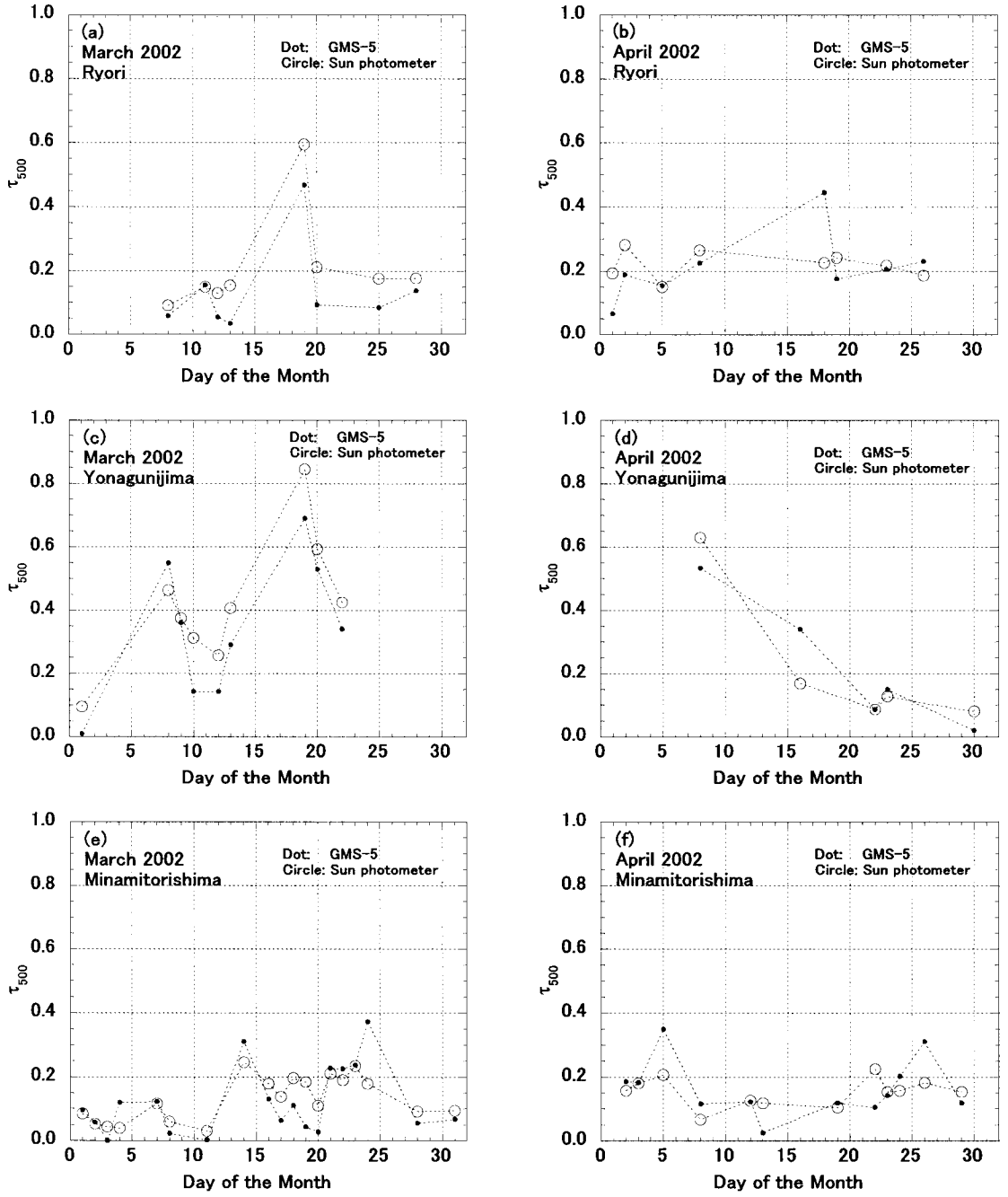

Fig. 2. Comparison of the daily AOT at 500 nm (τ_{500}) derived from the GMS-5 and the sun photometer measurements.
(a) Ryori, March 2002, (b) Ryori, April 2002, (c) Yonagunijima, March 2002, (d) Yonagunijima, April 2002, (e) Minamitorishima, March 2002, (f) Minamitorishima, April 2002.

vation sites, comparing the GMS-5 derived daily AOT with those from the sun photometer measurements taken in March and April 2002. Correlation coefficients (and the number of sample days) are 0.74 (16), 0.91 (14), 0.69 (31), and 0.85 (61) for Ryori, Yonagunijima, Minamitorishima, and the sum of all observation sites, respectively.

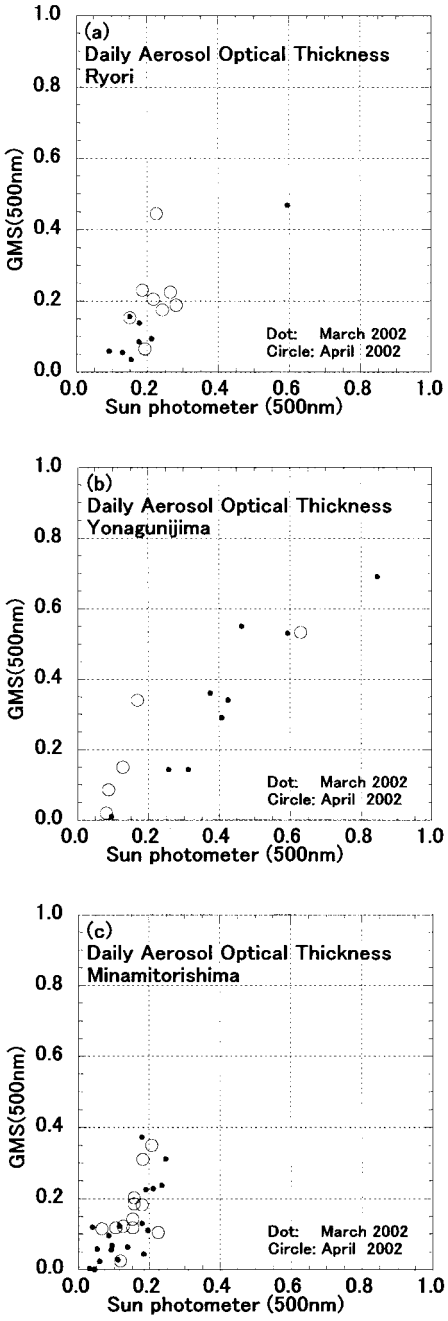

Fig. 3. Scatter plot of the daily AOT at 500 nm; sun photometer vs GMS-5. (a) Ryori, (b) Yonagunijima, and (c) Minamitorishima.

From these results, we can conclude that the GMS-5 derived daily AOT roughly agrees with that determined from the sun photometers. The differences are mainly caused by the following facts; (1) we used a typical dust model to retrieve AOT from the GMS-5 while the scattering properties of aerosols over the ocean varies according to the origin and the transporting process and (2) the observational time and the location to derive the daily AOTs are different between the GMS-5 and the sun photometers.

It is noticed from Fig. 2(a), that AOT is very large at Ryori station on 19 March 2002 while it drastically decreases on the next day. Similar trend is also seen at Yonagunijima station [Fig. 2(c)]. The daily AOT distributions derived from the GMS-5 measurements on 19～20 March 2002 are displayed in Figs. 4(a) and 4(b), where land and cloudy areas are shown in black. Total column mass concentrations of dust particles, which were produced by the Model of Aerosol Species in the Global Atmosphere (MASINGAR) (Tanaka and Chiba 2005), are presented in Figs. 4(c) and 4(d) for a comparison purpose. Because the GMS-5 has only one broad-band channel in the visible wavelength region, it is impossible to distinguish dust aerosols from other aerosol types. Thus, the GMS-5 derived AOT map displays all aerosol types. On the other hand, the MASINGAR can treat various aerosol types separately. The dust type aerosols are displayed in Figs. 4(c) and 4(d).

Heavy dust area is simulated by the MASINGAR in the middle of the Sea of Japan on 19 March 2002. It spreads out easterly beyond the Honshu island of Japan. In the GMS-5 derived AOT distribution map, heavy dust area is also observed in the same region. Aerosols with large AOT observed at Ryori station is most probably composed of dust particles. On the other hand, aerosols with large AOT near Yonaginijima may be composed of other types of aerosols. On 20 March 2002, dust area is simulated by the MASINGAR from the Korean Peninsula to the Pacific Ocean across the Japan islands. This dust belt is also shown clearly in the AOT distribution map derived from the GMS-5 measurements.

3.2 Monthly aerosol optical thickness

Figure 5 shows monthly AOT distributions over the ocean, derived from the GMS-5 measurements in March and April of 2002 and 2003. As can be seen in Figs. 4(a) and 4(b), cloud screening is not necessarily perfect near clouds. The retrieved AOT might be overestimated in such cases. To reduce the influ-

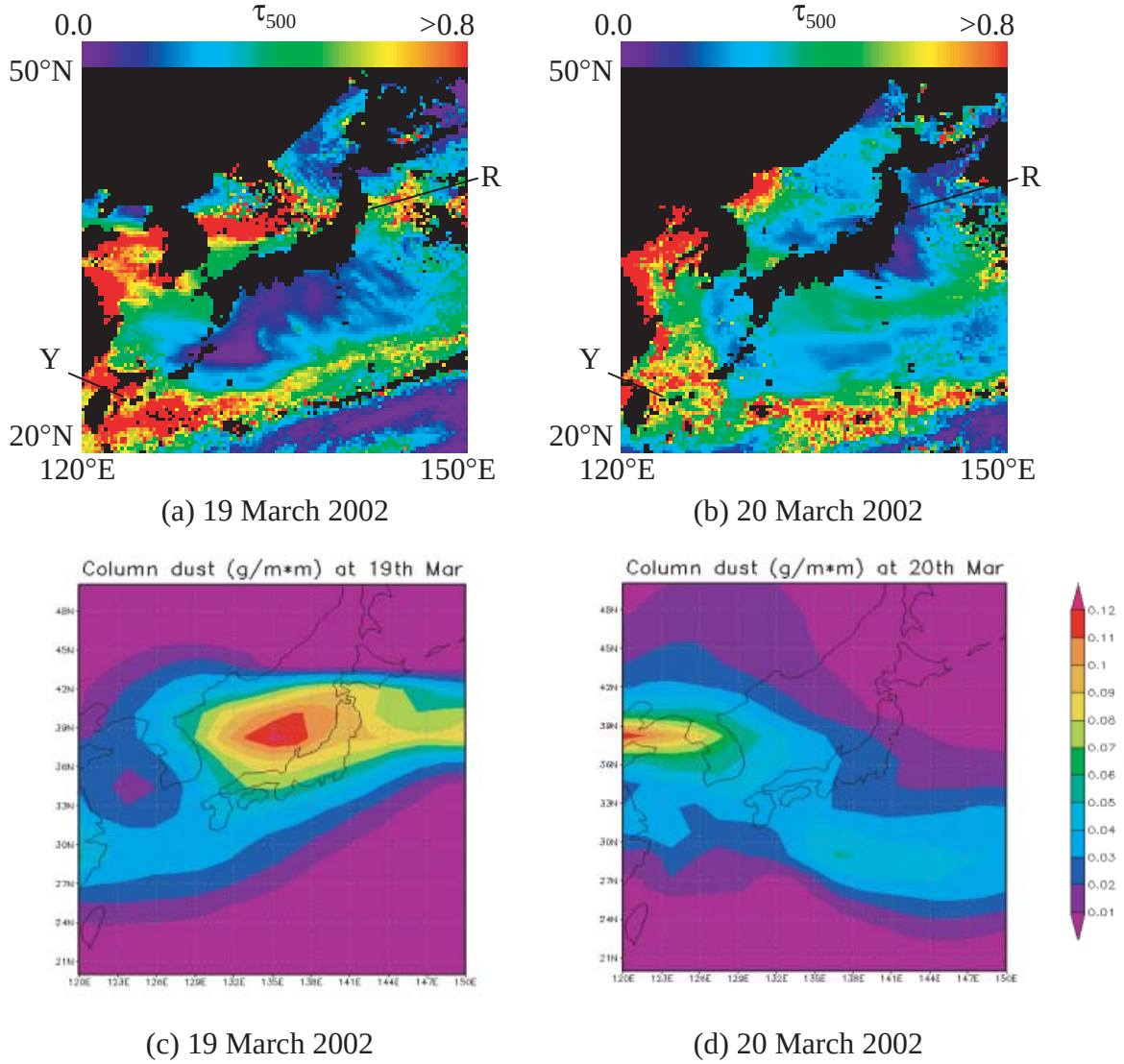

Fig. 4. (a) Daily AOT at 500 nm (τ_{500}) derived from the GMS-5 on 19 March 2002. (b) The same as (a) but for 20 March 2002. (c) Total column dust mass concentration simulated by the MASINGAR on 19 March 2002. (d) The same as (c) but for 20 March 2002. The symbols R and Y denote Ryori and Yonagunijima, respectively.

ence of these uncertain data, the monthly AOT is obtained as the median of the daily AOTs rather than the mean at each grid, because the median is more robust estimator than the mean for broad distribution with outlier data.

The highest AOT is observed over the Yellow Sea and the East China Sea. There could be, however, an influence of higher segment and pigment concentrations in the ocean typical around these areas. AOT might consequently be overestimated due to the radiation reflected by such segments and pigments. Aerosol area with the optical thickness of 0.3∼0.6 is observed over the midlatitude of the Pacific Ocean in the northern hemisphere (>30°N). Moderately thick aerosol area (∼0.3) is noticed around the 10°N except for April 2002. There is a very low AOT belt over the equatorial area. Similar pattern of the AOT is also presented in the near real time monthly global images (Level-3 products) derived from the Moderate Resolution Imaging Spectroradi-

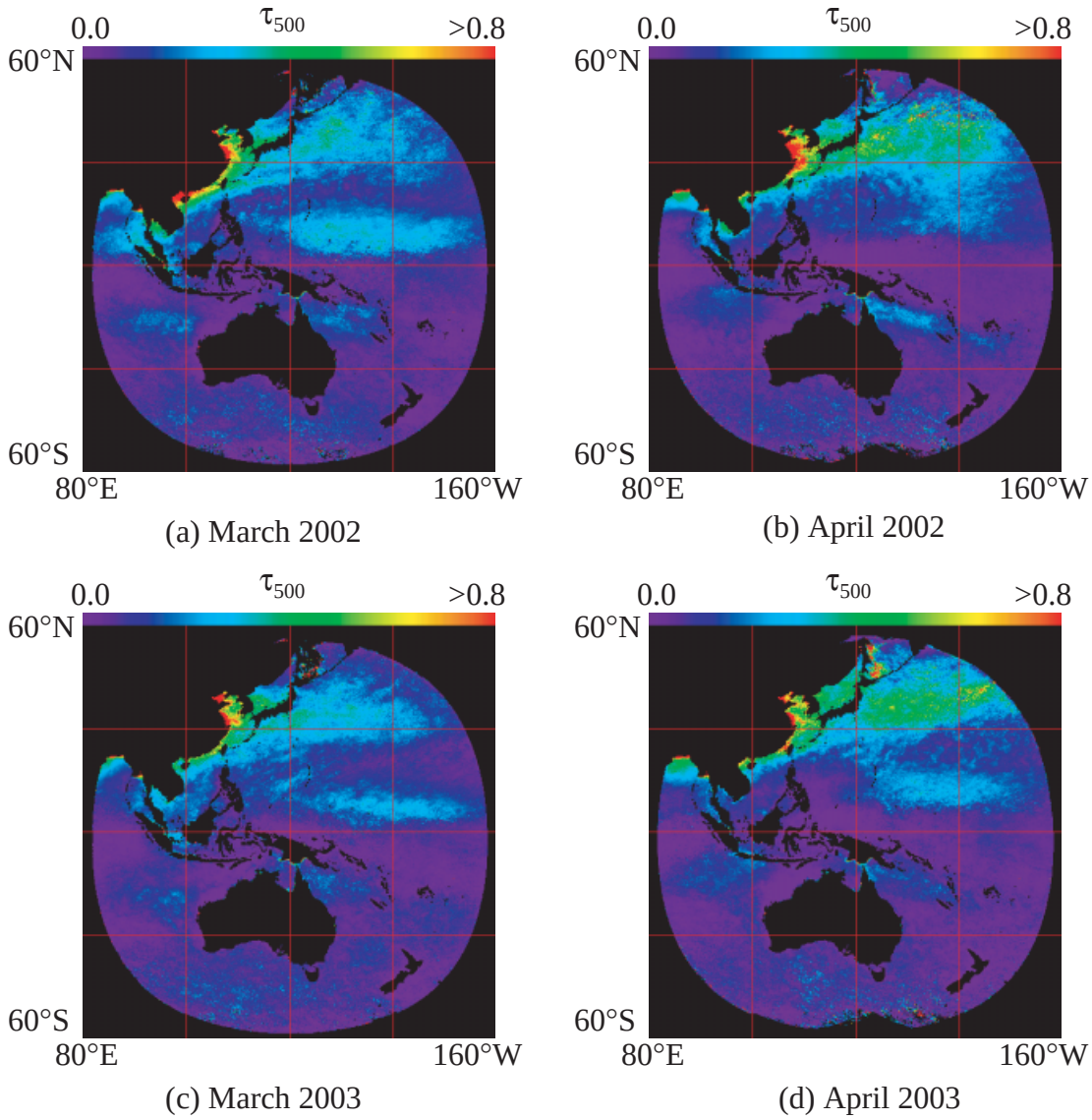

Fig. 5. Monthly AOT at 500 nm (τ_{500}) derived from the GMS-5. (a) March 2002, (b) April 2002, (c) March 2003, (d) April 2003.

ometer (MODIS) onboard Terra satellite, which is open to the public through National Aeronautics and Space Administration/Goddard Space Flight Center via World Wide Web. It is of interest to note that moderately thick aerosols exist around 10°N. But investigating the origin of such aerosols is beyond the scope of this paper.

Table 1 shows the monthly AOT near the sun photometer sites in March and April of 2002 and 2003. These values are obtained as the median of the daily AOTs in a 4×4 grid area near the sun photometer observation site. The total number of daily AOT used to obtain the monthly AOT is presented in parentheses. In March, remarkable differences are not seen between 2002 and 2003. In April, about 20% of change in AOT are noticed between 2002 and 2003 at Ryori and Minamitorishima stations. The monthly mean AOTs in March and April 2002, reported in JMA (2004), is shown for comparison purposes. The differences of retrieved monthly AOT, the GMS-5 minus the sun photometer, in March and April are −0.03

Table 1. Monthly aerosol optical thickness at 500 nm, retrieved from the GMS-5 and the sun photometer measurements

Station	GMS-5	Sun photometer	GMS-5	Sun photometer
	March 2002		April 2002	
Ryori	0.18 (374)*	0.21	0.27 (348)	0.24
Yonaguni-jima	0.40 (256)	0.41	0.40 (258)	0.22
Minami-torishima	0.14 (458)	0.13	0.22 (478)	0.15
	March 2003		April 2003	
Ryori	0.17 (370)	—	0.33 (313)	—
Yonaguni-jima	0.39 (159)	—	0.39 (224)	—
Minami-torishima	0.14 (448)	—	0.18 (458)	—

*Total number of grids used to obtain the GMS-5 monthly AOT.

and 0.03 at Ryori, −0.01 and 0.18 at Yonagunijima, and 0.01 and 0.07 at Minamitorishima, respectively. These differences are partly caused by the fact that the days for calculating the monthly AOTs are not necessarily the same between the GMS-5 and the sun photometers.

Regional monthly AOT is presented in Table 2(a) for March and April of 2002 and 2003. The observation area (Fig. 5) is divided into regions of 30° latitude and 30° longitude. The total number of daily AOTs used to obtain these values is shown in Table 2(b). As mentioned before, AOT might be overestimated over the ocean near the Asian continent due to the influence of the segment and pigment concentrations. To reduce the influence of such uncertain AOTs, regional monthly AOT is obtained as the median of the AOTs in each region rather than the mean.

As expected, the largest AOT (about 0.4∼0.5) is found in the western part of the 30°N∼60°N latitudes. In these latitudes, AOT decreases as the longitude increases, and AOTs are larger in April than in March by ∼0.1. In the 0°N∼30°N, the monthly AOTs are about 0.1∼0.2. AOTs in the southern hemisphere are less than 0.1, but AOT in the 0°S∼30°S is a little bit smaller than that in the 30°S∼60°S on average.

The AOTs in 2003 seem to be smaller than those in 2002 in six regions from 110°E to 160°W of the northern hemisphere, where the Asian dust is most likely to affect the aerosol loading. The numbers of regions, in which the AOT increased/decreased/equivalent from 2002 to 2003, are 3/8/1 for March and April from 110°E to 160°W of the northern hemisphere, and the changes in AOT from 2002 to 2003 are as large as −0.04∼0.03. It is reported that the spring dust events in 2002 were remarkably strong, while not so much in 2003. The annual trend presented in the GMS-5 derived AOT is generally consistent with these facts. However, further investigations are necessary to assess the relationship between satellite derived AOT, and the frequency and strength of dust events.

4. Sensitivity of the inversion method

The model aerosol used for retrieving AOT consists only of dust particles, which are situated in the 2∼5 km layer (Section 2). Thus, the GMS-5 retrieved AOT is the equivalent value, which is derived on the assumption that the aerosols over the ocean have the same optical properties as the modeled dust aerosols. Furthermore, the column water vapor amount is fixed as 2.9 cm, of which the variance may affect the upward radiation at the top of the atmosphere. Accuracy of retrieval could be therefore influenced by these model assumptions.

In this section, we examine the AOT retrieval errors caused by the assumptions of aerosol model, aerosol layer altitude, and column water vapor amount. Hereafter, we refer to the atmosphere model described in Section 2 as “reference model” or “RF model”. We will prepare synthesized measurement (pseudo-satellite measurement) from the radiative transfer calculations for various modified atmosphere models. The AOT for the synthesized measurement is then retrieved by referring to the look-up table, which was created using the reference model.

Nagai et al. (2004) reported that the dust layers with a thickness of 2∼3 km are observed between the altitude of 0∼8 km from the lidar measurements at Tsukuba (36.1°N, 140.1°E) and Naha (26.2°N, 127.7°E), Japan in March

Table 2. (a) Monthly regional AOT at 500 nm derived from the GMS-5, (b) Total number of grids used to obtain the monthly regional AOT

(a)

	March 2002				April 2002			
	80°E~110°E	110°E~140°E	140°E~170°E	170°E~160°W	80°E~110°E	110°E~140°E	140°E~170°E	170°E~160°W
30°N~60°N	—	0.38	0.25	0.19	—	0.47	0.34	0.29
0°N~30°N	0.22	0.17	0.19	0.16	0.14	0.12	0.16	0.14
0°S~30°S	0.09	0.05	0.09	0.05	0.06	0.04	0.06	0.05
30°S~60°S	0.09	0.09	0.09	0.04	0.08	0.09	0.08	0.04
	March 2003				April 2003			
	80°E~110°E	110°E~140°E	140°E~170°E	170°E~160°W	80°E~110°E	110°E~140°E	140°E~170°E	170°E~160°W
30°N~60°N	—	0.40	0.22	0.17	—	0.44	0.35	0.28
0°N~30°N	0.16	0.17	0.16	0.12	0.17	0.09	0.17	0.12
0°S~30°S	0.06	0.05	0.08	0.05	0.08	0.05	0.06	0.05
30°S~60°S	0.06	0.09	0.09	0.05	0.06	0.09	0.06	0.03

(b)

	March 2002				April 2002			
	80°E~110°E	110°E~140°E	140°E~170°E	170°E~160°W	80°E~110°E	110°E~140°E	140°E~170°E	170°E~160°W
30°N~60°N	0	65,027	163,308	60,769	0	59,069	145,711	50,087
0°N~30°N	136,770	285,661	341,599	245,764	116,968	300,436	330,846	256,395
0°S~30°S	224,686	157,121	180,860	202,261	238,912	160,255	232,075	220,835
30°S~60°S	69,766	138,536	161,268	80,306	57,528	127,324	123,405	69,408
	March 2003				April 2003			
	80°E~110°E	110°E~140°E	140°E~170°E	170°E~160°W	80°E~110°E	110°E~140°E	140°E~170°E	170°E~160°W
30°N~60°N	0	59,963	166,791	63,381	0	57,965	154,422	52,774
0°N~30°N	127,828	286,361	359,212	284,406	124,832	293,591	328,230	249,318
0°S~30°S	257,435	140,765	199,533	204,957	208,938	161,220	227,594	216,070
30°S~60°S	69,922	162,383	172,449	73,944	75,601	149,067	127,573	63,181

2003. The altitude of dust layer in the reference model (2~5 km) is not so different from these results. However, the thickness and the altitude of dust layer possibly change during the transportation. We modified the altitude of dust layer from the 2nd layer (2~5 km) in the RF model to the 1st layer (0~2 km) (referred to as "A1" model) and the 3rd layer (5~13 km) (referred to as "A3" model) without changing other parameters.

To estimate the effect of the column water vapor amount, we modified the atmospheric molecular model from the midlatitude summer model used in the RF model to the tropical model of which the column water vapor amount is 4.2 cm (referred to as "TR" model) or the subarctic winter model of which the column water vapor amount is 0.4 cm (referred to as "SW" model).

Aerosol modeling is more difficult compared with the altitude of aerosol layer and the column water vapor amount. The optical proper-

ties of aerosols are significantly dependent on the size distribution, the refractive index, and particle shapes. Furthermore, these parameters could not change independently. For example, the size distribution parameters and the refractive index may be altered by a change of the ambient atmospheric relative humidity (Shettle and Fenn 1979). In this paper, the effects of the variation in these parameters are not examined explicitly. Instead, sensitivity tests are performed by using basic aerosol component models to get a grasp of the accuracy in the AOT retrieval. According to Radiation Commission reports (WCP-55, 1983, WCP-112, 1986), basic components of the maritime aerosols are generally the "oceanic" model for particles generated at the sea surface and the "water soluble" model for aerosols soluble in water and consisting of a mixture of sulfate, nitrate, and organic components. The aerosol models used in this section are the oceanic (OC) model of log-normal size distribution with the (r_m, σ) values of (0.3 μm and 2.51) (WCP-112, 1986), and the water soluble (WS) model with (0.0285 μm and 2.239) (WCP-55, 1983). The refractive indices at a wavelength of 690 nm, for which the single scattering calculations are performed, is $1.38\text{-}i4.68 \times 10^{-8}$ for the OC model, and $1.53\text{-}i6.93 \times 10^{-3}$ for the WS model. Single scattering properties for these aerosol models are calculated by Mie scattering theory on the assumption that these aerosols are composed of spherical particles. Single scattering phase functions of the aerosol models (OC, WS, and RF) are illustrated in Fig. 6. The atmospheric model including the OC aerosols in the 0∼2 km layer and that including the WS aerosols in the 0∼2 km layer are used for comparisons. Note that we use abbreviations (RF, WS, and OC) to denote both aerosol models themselves and atmospheric models including the aerosol models.

Figure 7 shows the upward reflectance at the top of the atmosphere as a function of AOT for the atmospheric models described above, in a specific solar, satellite, and target pixel geometry. Figures 7(a), 7(b), and 7(c) show the effects of the altitude of aerosol layer, the column water vapor amount, and the aerosol model, respectively. From these results, we can conclude that the retrieval errors due to the change of aerosol layer altitude can be practically negligible and that a precise column water vapor amount is important only when an accurate aerosol model is used in the inversion process. Hereafter, we focus on the influence of aerosol model assumption on the AOT retrieval.

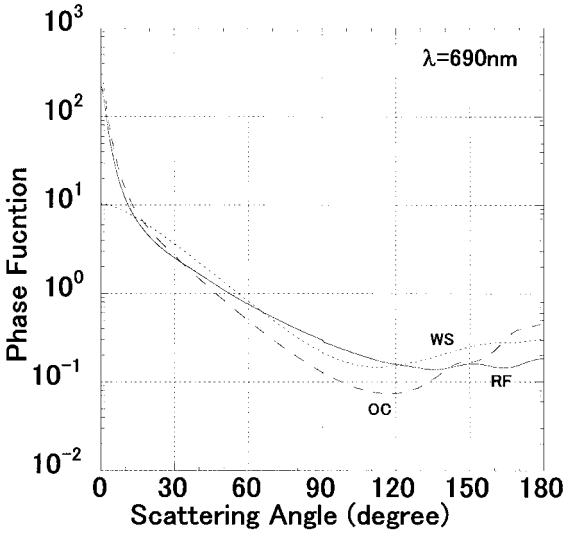

Fig. 6. Single scattering phase functions of model aerosols. RF, WS, and OC denote the reference model, the water soluble model, and the oceanic model, respectively.

Figure 8 shows AOT retrieval errors when the RF model is applied to the synthesized data which are generated for the OC and for the WS models. Three cases of solar, satellite, and target pixel geometries are shown. Corresponding scattering angles (Θ) are 124°, 152°, and 163° from the top to the bottom. It should be noted that passive satellite remote sensing is usually made from the side scattering to the back scattering angle ranges. For example, the scattering angle varies from 125° to 175° at Ryori, Yonagunijima, and Minamitorishima observation sites during 09 JST and 15 JST in March and April for the GMS-5 observation.

In Fig. 7(c), the τ_{500} values for the reflectance of 0.047 are 0.16 and 0.33 for the OC and the RF models, respectively. In this case, τ_{500} is overestimated by 0.17 when the RF model is applied to the synthesized data using the OC model. This value is plotted at the abscissa of $\tau_{500} = 0.16$ in Fig. 8(c).

Reflectance at the top of the atmosphere is strongly related to the product of the albedo for

single scattering (ω_0) and the single scattering phase function. The ω_0 values are 0.90, 1.00, and 0.96 for the RF model, the OC model, and the WS model, respectively. In the followings, we roughly analyze the retrieval errors presented in Fig. 8, by referring to the single scattering phase function of aerosol models (Fig. 6) and the ω_0 values.

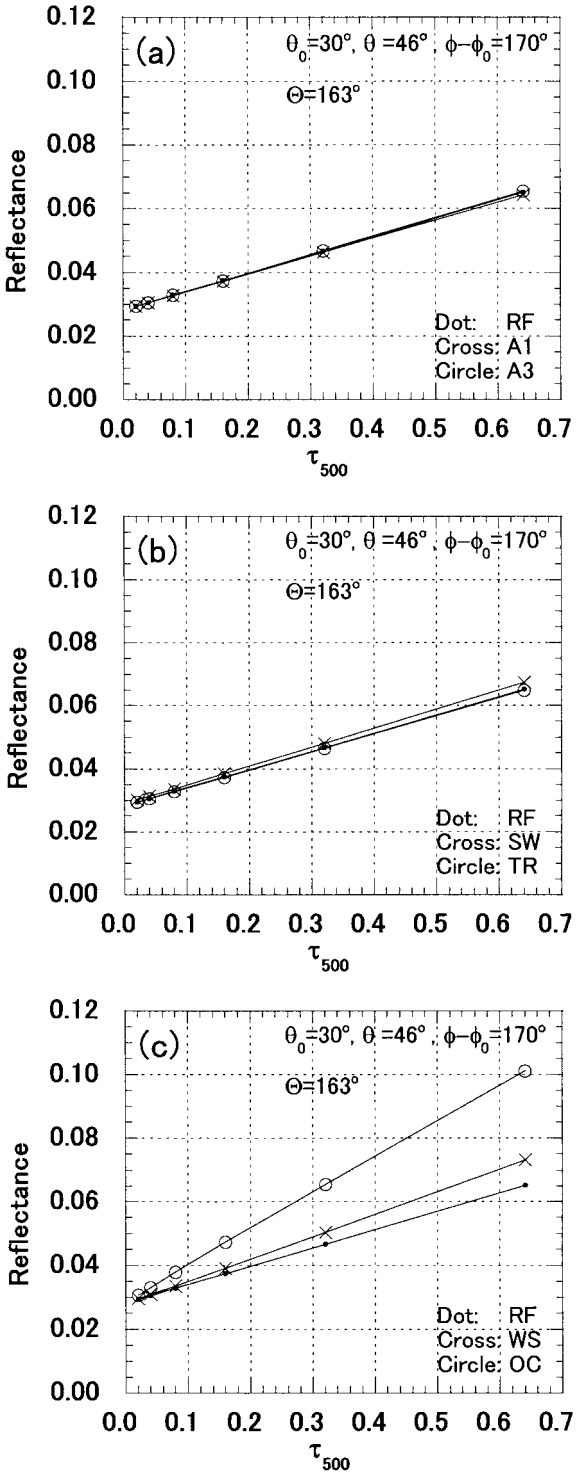

Fig. 7. Reflectance at the top of the atmosphere as a function of aerosol optical thickness (τ_{500}).
(a) the effect of the altitude of aerosol layer, dot: RF (2∼5 km), cross: A1 (0∼2 km), circle: A3 (5∼13 km).
(b) the effect of the column water vapor amount, dot: RF (2.9 cm), cross: SW (0.4 cm), circle: TR (4.2 cm).
(c) the effect of aerosol model assumption, dot: RF, cross: WS, circle: OC. θ_0, solar zenith angle; θ, satellite zenith angle; $\phi - \phi_0$, azimuth difference angle; Θ, scattering angle.

The single scattering phase function of the WS model is larger than that of the RF model in the scattering angle range from 120° to 170° (Fig. 6), and ω_0 of the WS model is also larger than that of the RF model. The reflectance generated using the WS model is consequently larger than that of the RF model as shown in Fig. 7(c). The differences in the reflectance cause an overestimate of the retrieved AOTs as shown in Figs. 8(a)∼8(c).

The reflectance for the OC model is much larger than the WS model at $\Theta = 163°$ [Fig. 7(c)]. Since the magnitude of single scattering phase function is approximately the same between the OC and the WS models at this scattering angle (Fig. 6), this reflectance difference is caused by the difference of ω_0. The AOT for the OC model is overestimated much larger than the WS model as shown in Fig. 8(c). The magnitude of single scattering phase function of the OC model is very similar to that of the RF model at $\Theta = 152°$, which is the scattering angle corresponding to Fig. 8(b). Due to the large ω_0 for the OC model, the reflectance is still larger than the RF model (not shown). The AOT is consequently overestimated as shown in Fig. 8(b). The magnitude of the single scattering phase function for the OC model is about the half of the RF model at $\Theta = 124°$, which is the scattering angle corresponding to Fig. 8(a). However, reflectance for the OC model is not so small compared to the RF model (not shown) due to the large ω_0. Retrieved AOT is a little bit

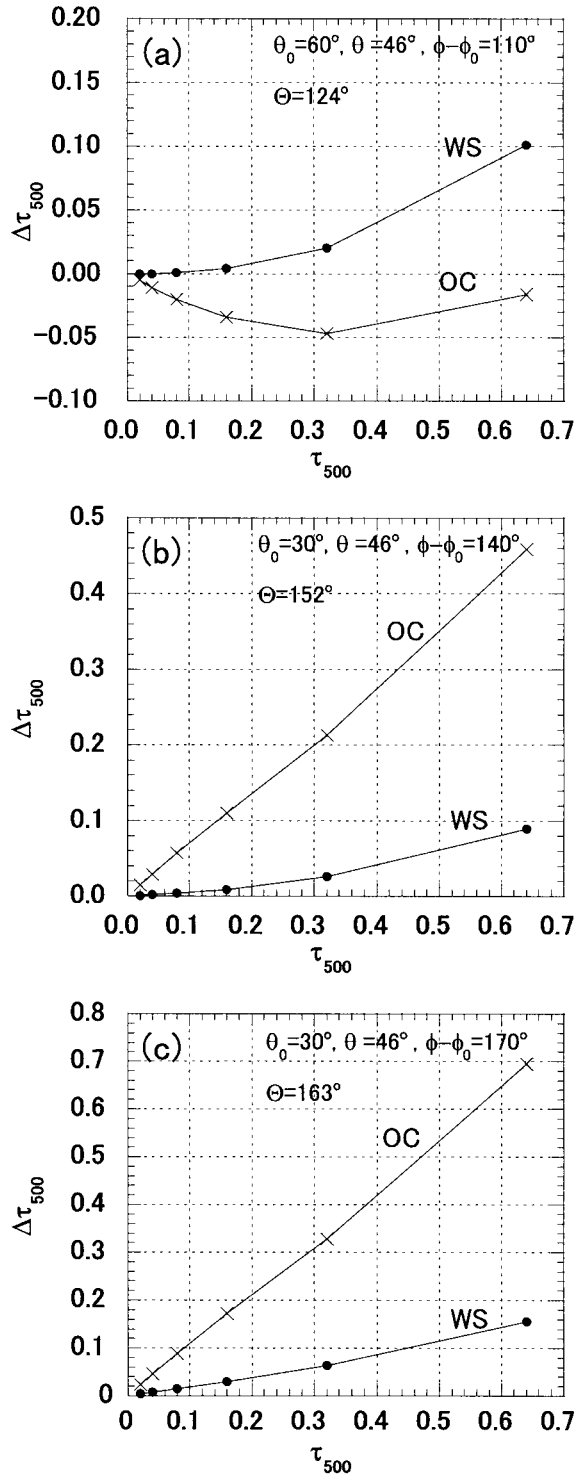

Fig. 8. AOT retrieval errors caused by the aerosol model assumption as a function of aerosol optical thickness (τ_{500}). θ_0, solar zenith angle; θ, satellite zenith angle; $\phi - \phi_0$, azimuth difference angle; Θ, scattering angle.

underestimated in this case as shown in Fig. 8(a).

ω_0 value is greatly dependent on the imaginary part of the refractive index of aerosols. To reduce the uncertainty in AOT retrieval from satellite visible data, a precise knowledge on the imaginary part of aerosol refractive index is very beneficial (Masuda et al. 2002a). It should be emphasized that the error analyses described in this section are based on simple aerosol models. To precisely examine the error budget in satellite retrieved AOT, a more realistic aerosol models should be included, for example, by taking into account the nonsphericity of sea salt aerosols (von Hoyningen-Huene and Posse 1997), and absorptive aerosols originating from biomass burning. The results presented in this section, however, might be useful as a guideline of the accuracy of AOT derived from one-channel AOT retrieval algorithm.

5. Summary and conclusions

To retrieve AOT from visible data of the GMS-5, atmospheric parameters, except for the AOT itself, have to be assumed because it has only one broad-band channel in the visible wavelength region. Furthermore, a 6-bit digitization in the visible channel is much worse than currently operating polar-orbiting satellites such as the MODIS. Nevertheless, geostationary satellites have an advantage over the polar-orbiting satellites in the capacity to provide a highly temporal resolution. Daily AOT distributions like Figs. 4(a) and 4(b) can be easily obtained from the hourly AOTs retrieved from geostationary satellite measurements, for example, by averaging them.

In the previous paper (Masuda et al. 2002b), we demonstrated that the accuracy of dust optical thickness over the ocean retrieved from the visible data of GMS-5 could be much improved by taking the nonsphericity of dust particles into account. In this paper, we further examined the AOT retrieval errors caused by the assumptions of aerosol model, aerosol layer altitude, and column water vapor amount. In the sensitivity test, single scattering properties for the aerosols were calculated by Mie scattering theory, for simplicity, on the assumption that the aerosols are composed of spherical particles. Computational results showed that the aerosol modeling, such as size distribution

and single scattering albedo, is much important than the aerosol layer altitude and the column water vapor amount for the AOT retrieval from the GMS-5 visible data.

The daily and monthly AOTs retrieved from the GMS-5 visible data were compared with those determined from the sun photometer measurements made by the Japan Meteorological Agency. The correlation coefficient between the GMS-5 and the sun photometer derived daily AOTs was 0.85 for 61 samples in March and April 2002 at three sun photometer observation sites (Ryori, Yonagunijima, and Minamitorishima.) in Japan. The differences of retrieved monthly AOT, the GMS-5 minus the sun photometer, in March and April 2002 were −0.03 and 0.03 at Ryori, −0.01 and 0.18 at Yonagunijima, and 0.01 and 0.07 at Minamitorishima, respectively.

Monthly regional AOT, defined as the median of the daily AOTs over a $30^\circ \times 30^\circ$ ocean area, were calculated using the GMS-5 measurements in latitude from 60°N to 60°S and longitude from 80°E to 160°W in March and April of 2002 and 2003. In the southern hemisphere, the monthly regional AOT was less than 0.1; about 0.1∼0.2 in 0°N∼30°N; and larger than 0.2 in 30°N∼60°N with a maximum of 0.4∼0.5 in the western region near the Asian continent.

The monthly regional AOT retrieved from the GMS-5 in 2003 were generally smaller than those in 2002 for six regions between 110°E and 160°W in the northern hemisphere, where the Asian dust is most likely to affect the aerosol loading. The numbers of regions in which the AOT increased/decreased/equivalent from 2002 to 2003 are 3/8/1. The changes in AOT from 2002 to 2003 were as large as −0.04∼0.03 in those regions. To assess the relationship between the satellite derived AOT, and the frequency and strength of dust events, further investigations are necessary.

Acknowledgments

This study is made as a part of the ADEC Project (Aeolian Dust Experiment on the Climate Impact) sponsored by the Ministry of Education, Culture, Sports, Science and Technology, the Japanese Government. Sun photometer measurement data were provided by the Japan Meteorological Agency. M. Chiba has provided us with the dust distribution maps produced by the MASINGAR. We sincerely thank M. Mikami and A. Uchiyama for their useful discussions. We would like to acknowledge the constructive criticisms from anonymous reviewers.

References

Cox, C. and W. Munk, 1954: Statistics of the sea surface derived from sun glitter. *J. Mar. Res.*, **13**, 198–227.

d'Almeida, G.A., P. Koepke, and E.P. Shettle, 1991: *Atmospheric Aerosols Global climatology and radiative characteristics*. A. Deepak Publishing, 561pp.

Higurashi, A. and T. Nakajima, 1999: Development of a two-channel aerosol retrieval algorithm on a global scale using NOAA AVHRR. *J. Atmos. Sci.*, **56**, 924–941.

Japan Meteorological Agency, 2004: *Annual report on atmospheric and marine environment monitoring*, No. 4, March 2004 (CD-ROM) (in Japanese with English summary).

Kneizys, F.X., E.P. Shettle, L.W. Abreu, J.H. Chetwynd, G.P. Anderson, W.O. Gallery, J.E.A. Selby, and S.A. Clough, 1988: *Users guide to LOWTRAN7*. Air Force Geophysics Laboratory Rep. AFGL-TR-88-0177, Hanscom AFB, MA, 146pp.

Masuda, K., H. Ishimoto, and T. Takashima, 2002a: Dependence of the spectral aerosol optical thickness retrieval from space on measurement errors and model assumptions. *Int. J. Remote Sens.*, **23**, 3835–3851.

———, Y. Mano, H. Ishimoto, M. Tokuno, Y. Yoshizaki, and N. Okawara, 2002b: Assessment of the nonsphericity of mineral dust from geostationary satellite measurements. *Remote Sens. Environ.*, **82**, 238–247.

———, ———, ———, ———, ———, ———, R. Yamagiwa, A. Uchiyama, A. Yamazaki, and Y. Tsutsumi, 2003: Comparisons of the mineral dust optical thickness retrieved from geostationary satellite with ground based radiometer measurements. *Remote Sens. Environ.*, **85**, 484–488.

Mikami, M., O. Abe, M. Du, O. Chiba, K. Fujita, M. Hayashi, Y. Iwasaka, K. Kai, K. Masuda, T. Nagai, T. Ootomo, J. Suzuki, A. Uchiyama, S. Yabuki, Y. Yamada, M. Yasui, G. Shi, X. Zhang, Z. Shen, W. Wei, and J. Zhou, 2002: The impact of Aeolian dust on climate: Sino-Japanese cooperative project ADEC. *J. Arid Land Studies*, **11**, 211–222.

Nagai, T., M. Nakazato, T. Matsumura, Y. Hirose,

and T. Sakai, 2004: Lidar observations of Aeolian dust vertical profiles over Tsukuba and Naha, Japan. *Proceedings of the 22nd International Laser Radar Conference (ILRC 2004)*, Matera, Italy 12–16 July 2004, 919–922.

Nakajima, T., M. Tanaka, M. Yamano, M. Shiobara, K. Arao, and Y. Nakanishi, 1989: Aerosol optical characteristics in the yellow sand events observed in May, 1982 at Nagasaki—Part II Models. *J. Meteor. Soc. Japan*, **67**, 279–291.

Pollack, J.B. and J.N. Cuzzi, 1980: Scattering by nonspherical particles of size comparable to a wavelength: a new semi-empirical theory and its application to tropospheric aerosols. *J. Atmos. Sci.*, **37**, 868–881.

Shettle, E.P. and R.W. Fenn, 1979: *Models for the aerosols of the lower atmosphere and the effects of humidity variations on their optical properties*. AFGL-TR-79-0214, Hanscom, AFB, MA, 94pp.

Tanaka, T.Y. and M. Chiba, 2005: Global simulation of dust aerosol with a chemical transport model, MASINGAR. *J. Meteor. Soc. Japan*, this issue.

von Hoyningen-Heune, W. and P. Posse, 1997: Nonsphericity of aerosol particles and their contribution to radiation forcing. *J. Quant. Spectrosc. Radiat. Transfer*, **57**, 651–668.

WCP-112, 1986: *A preliminary cloudless standard atmosphere for radiation computation*. WMO/TD-No. 24, World Meteorological Organization, Geneva, 53pp.

WCP-55, 1983: *Report of the expert meeting on aerosols and their climate effects*. edited by A. Deepak and H.E. Gerber, World Meteorological Organization, Geneva, 107pp.